Hyperspherical close-coupling calculations for electron-capture cross sections in low-energy $Ne^{10+}+H(1s)$ collisions

Patricia Barragán,* Anh-Thu Le, and C. D. Lin
Department of Physics, Kansas State University, Manhattan, Kansas 66506, USA
(Received 3 May 2006; published 26 July 2006)

We present total and partial electron-capture cross sections for $Ne^{10+}+H(1s)$ collisions at energies from 0.01 eV to 1 keV using the hyperspherical close-coupling method. Good agreements with the previous calculations by the classical-trajectory Monte-Carlo method are found for total capture cross section, but not for partial cross sections, especially below about 200 eV/amu. We found that the total cross section is mainly due to the population of $n=7$ channels and only at energies above 50 eV/amu $n=5,6$ channels begin to contribute to the total cross section.

DOI: 10.1103/PhysRevA.74.012720 PACS number(s): 34.10.+x, 34.70.+e, 31.15.Ja

I. INTRODUCTION

Electron-capture reactions between charged ions and atoms are important processes in fusion and astrophysical plasmas. In a fusion plasma, the charge-transfer reactions are used as diagnostic tools to measure density, temperature, and other parameters of the plasma. Moreover, they are employed to stimulate certain favorable conditions for the plasma [1]. In the case of astrophysical plasmas, several recent works have suggested that electron-capture processes are responsible for the heating of photoionized nebulae [2] and for x-ray emission from comets [3,4].

Experimentally it is rather difficult to measure low-energy electron-capture cross sections and the merged-beam technique has to be used [5]. Thus, reliable theoretical calculations are needed, and for low-energy collisions a fully quantal treatment of the scattering problem is required. In the last decades, several theoretical methods have been developed. Examples of published works using a common reaction coordinate (CRC) method can be found in [6–9]. In [10,11] the hyperspherical close-coupling (HSCC) method has been used. These calculations have been found to give accurate total electron-capture cross sections at low energies where comparison with experiments is possible. A comparison between the HSCC and CRC methods for the same collision system has been performed in [12], and general good agreement between the two approaches has been established.

In this paper we report on calculations performed for $Ne^{10+}+H(1s)$ collisions for center-of-mass energy from 0.01 eV to 1 keV. The processes are studied

$$Ne^{10+} + H(1s) \rightarrow Ne^{9+}(nl) + H^{+}. \tag{1}$$

In the case of the $Ne^{10+}+H(1s)$ electron-capture reaction, only a few works have been performed so far. Meyer *et al.* carried out measurements of total electron-capture cross sections at energies from 0.9 to 8 keV/amu [13]. In [14] a classical model was employed to calculate cross sections for $E=0.5-100$ keV/amu. In [15,16] the classical-trajectory Monte Carlo approach was used to obtain electron-capture cross sections in the intermediate- and high-energy regions. In [17], classical and semiclassical calculations have been performed for energies between 1 and 500 keV/amu. Pérez *et al.* [18] reported the only low-energy calculations. In that work, a classical trajectory Monte Carlo method was used to obtain electron-capture cross sections between 1 eV/amu and 100 keV/amu.

This paper is organized as follows. In Sec. II we summarize the HSCC method. In Sec. III we present our calculated electron-capture cross sections and compare them with previous works. In the last section we summarize the main conclusions. All the energies are given in the center-of-mass frame. Atomic units are used unless otherwise indicated.

II. HYPERSPHERICAL CLOSE-COUPLING METHOD

The hyperspherical method has been widely used in a variety of three-body systems [19]. We employed the HSCC method as described in [10] to calculate cross sections in ion-atom collisions for the reaction between Ne^{10+} and $H(1s)$.

The three particles in the quasimolecule $(NeH)^{10+}$ are described using hyperspherical coordinates. In the molecular frame there are three equivalent sets of Jacobi coordinates that can be used to describe the relative motions between particles. We choose $\boldsymbol{\rho}_1$ and $\boldsymbol{\rho}_2$ to be the vectors from Ne^{10+} to H^+ and from the center of mass of Ne^{10+} and H^+ to the electron, respectively. The reduced masses associated with these coordinates are μ_1 and μ_2. The hyperradius R and hyperangle ϕ are defined as

$$R = \sqrt{\frac{\mu_1}{\mu}\rho_1^2 + \frac{\mu_2}{\mu}\rho_2^2} \tag{2}$$

and

$$\tan\phi = \sqrt{\frac{\mu_2}{\mu_1}\frac{\rho_2}{\rho_1}}, \tag{3}$$

where μ is arbitrary. In this paper we chose $\mu=\mu_1$; thus, the hyperradius R becomes very close to the internuclear dis-

*Present address: Laboratorio asociado al CIEMAT de Física Atómica y Molecular en Plasmas de Fusión, Departamento de Química C-IX, Universidad Autónoma de Madrid, Madrid 28049, Spain. Electronic address: patricia.barragan@uam.es

tance between the two atoms in the collision. We also define the angle between the two Jacobi vectors as θ. First, we introduce the rescaled wave function

$$\Psi(R,\Omega,\hat{\omega}) = \psi(R,\Omega,\hat{\omega})R^{3/2}\sin\phi\cos\phi. \quad (4)$$

The Schrödinger equation then takes the form

$$\left(-\frac{1}{2}\frac{\partial}{\partial R}R^2\frac{\partial}{\partial R}+\frac{15}{8}+H_{\rm ad}(R,\Omega,\hat{\omega})-\mu R^2E\right)\Psi=0, \quad (5)$$

where $\Omega\equiv\{\phi,\theta\}$ and $\hat{\omega}$ denotes the three Euler angles $\{\omega_1,\omega_2,\omega_3\}$ of the body-fixed frame axes with respect to the space-fixed frame. $H_{\rm ad}$ is the scaled adiabatic Hamiltonian, defined by

$$H_{\rm ad}(R,\Omega,\hat{\omega}) = \frac{\Lambda^2}{2}+\mu RC(\Omega), \quad (6)$$

where Λ^2 is the square of the grand-angular momentum operator and C/R is the total Coulomb interaction between the particles.

To solve Eq. (5) the rescaled wave function is expanded in terms of the normalized and symmetrized rotation functions $\tilde{D}$. The body frame adiabatic basis functions $\Phi^A_{\nu I}(R,\Omega)$ are defined by

$$\Psi(R,\Omega,\hat{\omega}) = \sum_{\nu}\sum_{I}F_{\nu I}(R)\Phi^A_{\nu I}(R,\Omega)\tilde{D}^J_{IM_J}(\hat{\omega}), \quad (7)$$

where ν is the channel index, M_J is the projection of total angular momentum $\boldsymbol{J}$ along the space-fixed z axis, and I is the absolute value of the projection of $\boldsymbol{J}$ along the body-fixed z' axis, the axis between Ne^{10+} and H^+ ions.

To remove weak collision channels, thus to reduce the number of basis functions in the calculation, we used a diabatization technique as described in [20]. The adiabatic and diabatic representations are related by a unitary transformation

$$\Phi^D = C\Phi^A, \quad (8)$$

where Φ^D denotes diabatic channel functions and C is the unitary transformation matrix, which is chosen as the solution of the linear equation

$$\frac{dC}{dR}-CP=0, \quad (9)$$

where P is the radial couplings matrix:

$$P_{\lambda\nu} = \left\langle\Phi^A_\lambda\left|\frac{d}{dR}\right|\Phi^A_\nu\right\rangle. \quad (10)$$

To avoid the calculation of the radial couplings directly we approximate the derivative with respect to the hyperradius in Eqs. (9) and (10) by the simple difference. Thus, Eq. (9) becomes

$$C_{\lambda\nu}(R+\Delta R) = \sum_{\mu}C_{\lambda\mu}(R)\langle\Phi^A_\mu(R)|\Phi^A_\nu(R+\Delta R)\rangle \quad (11)$$

and the transformation matrix C can be obtained through the overlap matrix elements. In practice, we choose to approximately diabatize sharp avoided crossings only and thus limiting the summation in Eq. (11) to the few channels which have large overlap. The main advantage of this procedure is that we are able to discard channels that are weakly coupled to the main channels. These are the channels that are strongly coupled with the entrance channel and among themselves.

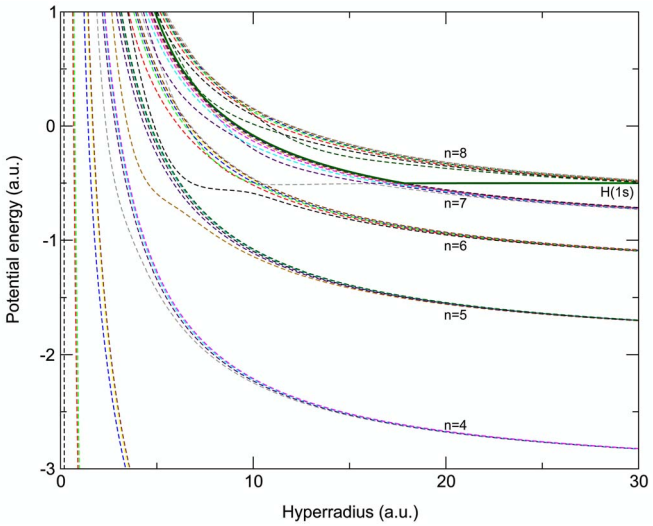

FIG. 1. (Color online) Adiabatic potential energy curves for $(NeH)^{10+}$. Only the $I=0$ channels from $n=4$ to $n=8$ are shown in addition to the entrance channel.

To solve the hyperradial equations we first divide the hyperradial space into sectors. We use the R-matrix propagation method [21] to propagate the R matrix from one sector to the next one up to a large hyperspherical radius R. We combine this method with the slow-smooth variable discretization (SVD) technique [22] in each sector. The electron-capture cross section for each partial wave J is then obtained from the scattering matrix $S^J_{\lambda\nu}$, and the total cross section from the initial state to the final state is given by the sum over all the partial-wave cross sections.

III. RESULTS

In order to obtain the potential energy curves of $(NeH)^{10+}$ for $I=0$ and $I=1$ we performed molecular calculations up to $R=30$ a.u. The calculation was extended up to $R=50$ a.u. to be able to obtain converged electron-capture cross sections at low energies. We calculated the adiabatic hyperspherical channel functions using B-spline basis functions. The adiabatic potential energy curves for $I=0$, from $n=4$ to $n=8$, are shown in Fig. 1. We observe that the most important avoided crossing occurs between the H(1s) entrance channel and $n=7$ channels. This suggests that $n=7$ channels will be the most populated in the collision between the Ne^{10+} ion and the H atom at low energies.

From the adiabatic curves we obtain the diabatic ones using the diabatization method described in Sec. II. We then select each channel from $n=5,6,7$ limits for $I=0$ and $I=1$, respectively, together with the entrance channel. This is the minimum set of seven channels to be included in the calculation, and these potential curves are shown in Fig. 2. Note that the reduction of channels can be done only after the

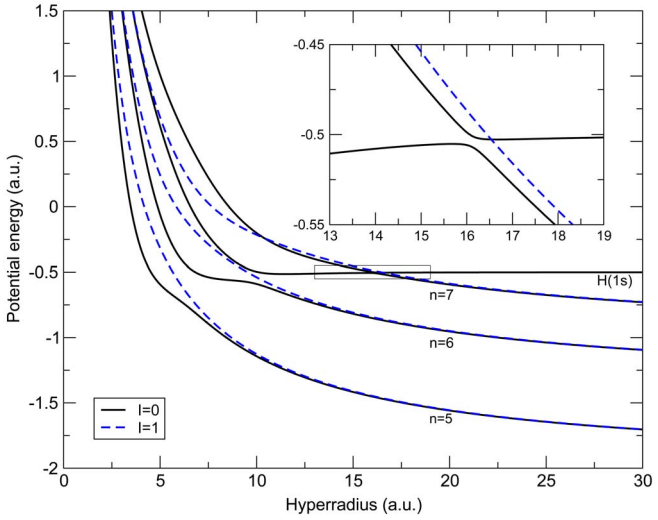

FIG. 2. (Color online) Selective seven diabatic potential energy curves of $(NeH)^{10+}$ used in the charge-transfer cross-section calculations. The solid lines are for $I=0$ and dashed lines for $I=1$. The inset shows the avoided crossing between the H($1s$) entrance channel and the first $I=0$ channel from $n=7$.

potential curves have been partially diabatized as described above. The inset of Fig. 2 illustrates that we do not diabatize all the avoided crossings (see the two solid curves). This avoided crossing at $R \simeq 16$ a.u. is responsible for the transition for charge transfer to the $n=7$ states at low energies. Note that the additional avoided crossings at smaller R's are expected to play an important role for electron capture to the $n=6$ and $n=5$ states at higher collision energies, respectively. The $I=1$ channels are included such that rotational coupling is included in the calculation.

In Fig. 3 we report our results for total and partial cross sections at center-of-mass energies between 0.01 eV and 1 keV. In the low-energy range, the cross section exhibits an approximate Langevin-type $1/v$ increase (see, for example,

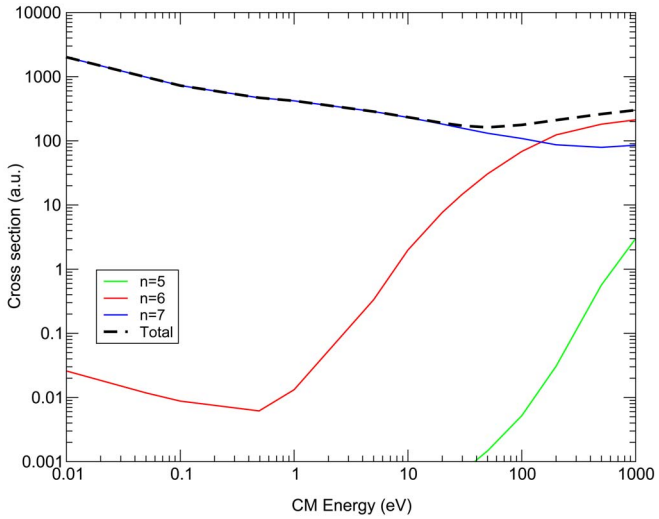

FIG. 3. (Color online) Results from the present calculation of the total and partial electron-capture cross sections for the reaction $Ne^{10+}+H(1s) \rightarrow Ne^{9+}(n)+H^+$.

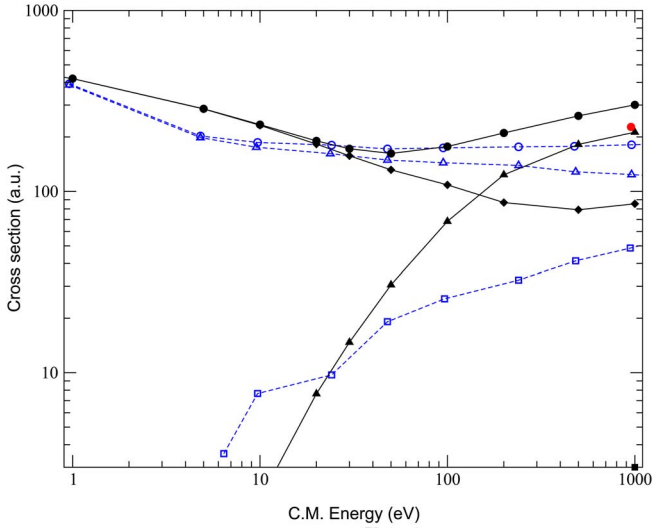

FIG. 4. (Color online) Comparison between the present calculated cross sections and previous results. Present results: (●) total, (▲) $n=6$, (♦) $n=7$. Pérez *et al.* [18]: (○) total, (□) $n=5$, (△) $n=6$. Meyer *et al.* [13]: (●) total.

[23,24]). The electron capture mainly occurs through transitions between the entrance channel and the $n=7$ capture channel at the avoided crossing at $R \simeq 16$ a.u. up to 30 eV. At energies above 30 eV, the $n=6$ cross section starts to be noticeable and becomes the dominant one above 100 eV. At 1 keV, we begin to see that $n=5$ is also populated.

We compare our results with those of previous works in Fig. 4. Experimentally only the total electron-capture cross sections are available. The low-energy point from Meyer *et al.* [13], as shown in the figure, is in good agreement with our calculation. The calculation of Pérez *et al.* [18] employed the classical-trajectory Monte Carlo method. Interestingly, even though this calculation gives total electron-capture cross sections that are nearly identical to the present quantum calculations, the partial cross sections are completely different from ours. In fact, their $n=6$ result is closer to our $n=7$ result, while their $n=5$ is closer to our $n=6$. It is not clear whether the figures in their paper for the n populations are mislabeled or there is a real difference between the classical versus quantum calculation.

In Fig. 5 we show the dependence of the cross section with impact parameter b at two energies of 50 eV (upper panel) and 500 eV (lower panel). The calculated partial-wave cross sections are converted to the impact parameter dependence through the relation $J=\mu b v$, where μ is the reduced mass of the system, b is the impact parameter, and v is the collision velocity. Note that electron capture to $n=7$ dominates at large impact parameters and capture to $n=6$ dominates at small impact parameters. An indication of the importance of the avoided crossing near $R \simeq 16$ a.u. for populating the $n=7$ is clearly seen since there is little probability for impact parameters greater than $b \simeq 16$ a.u. Similarly the $n=6$ channels are not populated for impact parameters beyond the avoided crossing at $R \simeq 10$ a.u.

To check the convergence of electron-capture cross sections with respect to the number of channels at high energy,

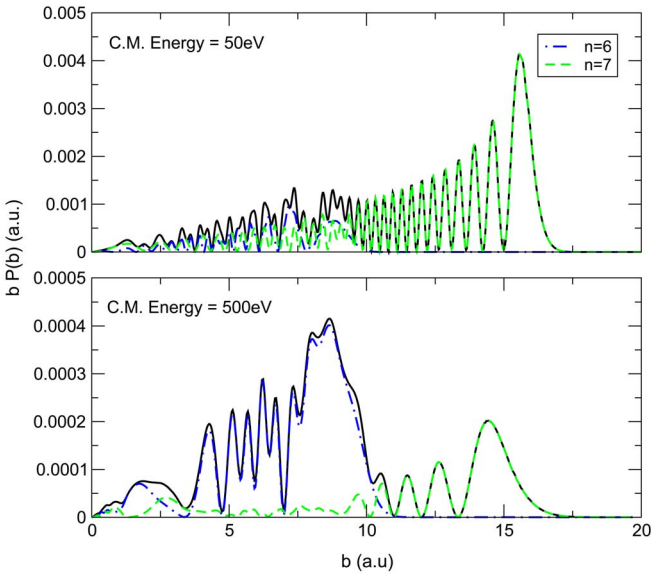

FIG. 5. (Color online) Dependence of the impact-parameter-weighted electron-capture probability $bP(b)$ with the impact parameter b at center-of-mass energies of 50 eV and 500 eV.

we have plotted the test results in Fig. 6 for the partial-wave cross sections for $E=1$ keV. The test consists of three calculations employing 7-, 17-, and 36-channel bases, respectively. The 17-channel basis set includes the first two channels from every n manifold, from $n=5$ to $n=8$ $(I=0,1)$, plus the initial state. The 36-channel basis includes the whole multiplets from $n=5$ to $n=7$ $(I=0,1)$ and the first channel with $n=8$ $(I=0,1)$, plus the initial state. As we can observe in Fig. 6, the most important differences among the three calculations take place at low J values. However, these discrepancies produce little differences (less than 10%) in the cross sections. From this calculation, we conclude that a 7-channel basis is enough to obtain the cross sections with the precision of a few percent.

IV. SUMMARY AND CONCLUSIONS

In this paper we have presented total and partial electron-capture cross sections for the collision system $Ne^{10+}+H(1s)$.

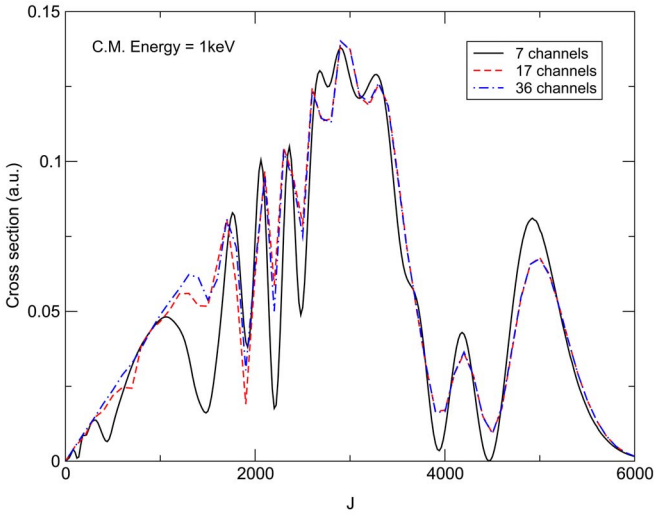

FIG. 6. (Color online) Test of the convergence of the electron-capture cross section with respect to the number of channels included in the calculation for a center-of-mass energy of 1 keV.

We have performed hyperspherical close-coupling calculations at center-of-mass energies between 0.01 eV and 1 keV. Our results for the total cross section agree with those of Pérez *et al.* [18] and Meyer *et al.* [13]. At low energy, our cross sections show that $n=7$ is the main populated channel. At energies above 50 eV, $n=5$ and $n=6$ become relevant. In the case of partial cross sections, there is a discrepancy with earlier classical-trajectory Monte Carlo calculations [18]. We have also studied the partial-wave dependence of the cross section and checked the convergence with respect to the number of channels, concluding that increasing from 7 to 36 channels produces negligible differences in the cross section.

ACKNOWLEDGMENTS

P.B. is grateful to the Spanish Ministry of Education and Science for a FPU grant and a "Estancia breve" at Kansas State University. This work is also supported by Chemical Sciences, Geosciences and Biosciences Division, Office of Basic Energy Sciences, Office of Science, U.S. Department of Energy.

[1] R. K. Janev, Phys. Scr. **96**, 94 (2002).
[2] J. B. Kingdon and G. J. Ferland, Astrophys. J. Lett. **516**, L107 (1999).
[3] C. M. Lisse, D. J. Christian, K. Dennerl, K. J. Meech, R. Petre, H. A. Weaver, and S. J. Wolk, Science **292**, 1343 (2001).
[4] T. E. Cravens, Science **296**, 1042 (2002).
[5] C. C. Havener, R. Rejoub, C. R. Vane, H. F. Krause, D. W. Savin, M. Schnell, J. G. Wang, and P. C. Stancil, Phys. Rev. A **71**, 034702 (2005).
[6] B. Herrero, I. L. Cooper, A. S. Dickinson, and D. R. Flower, J. Phys. B **28**, 711 (1995).
[7] P. Barragán, L. F. Errea, L. Méndez, A. Macías, I. Rabadán, and A. Riera, Phys. Rev. A **70**, 022707 (2004).
[8] P. Barragán, L. F. Errea, L. Méndez, I. Rabadán, and A. Riera, Astrophys. J. **636**, 544 (2006).
[9] P. Barragán, L. F. Errea, L. Méndez, I. Rabadán, and A. Riera, Phys. Rev. A (to be published).
[10] C. N. Liu, A. T. Le, T. Morishita, B. D. Esry, and C. D. Lin, Phys. Rev. A **67**, 052705 (2003).
[11] A. T. Le, M. Hesse, T. G. Lee, and C. D. Lin, J. Phys. B **36**, 3281 (2003).
[12] A. T. Le, C. D. Lin, L. F. Errea, L. Méndez, A. Riera, and B. Pons, Phys. Rev. A **69**, 062703 (2004).
[13] F. W. Meyer, A. M. Howald, C. C. Havener, and R. A. Phaneuf, Phys. Rev. A **32**, 3310 (1985).
[14] T. P. Grozdanov, J. Phys. B **13**, 3835 (1980).

[15] R. E. Olson and A. Salop, Phys. Rev. A **16**, 531 (1977).
[16] G. Maynard, R. K. Janev, and K. Katsonis, J. Phys. B **25**, 437 (1992).
[17] L. F. Errea, C. Illescas, L. Méndez, B. Pons, A. Riera, and J. Suárez, J. Phys. B **37**, 4323 (2004).
[18] J. A. Perez, R. E. Olson, and P. Beiersdofer, J. Phys. B **34**, 3063 (2001).
[19] C. D. Lin, Phys. Rep. **257**, 1 (1995).
[20] M. Hesse, A. T. Le, and C. D. Lin, Phys. Rev. A **69**, 052712 (2004).
[21] J. C. Light and R. B. Walker, J. Chem. Phys. **65**, 4272 (1976).
[22] S. W. O. I. Tolstikhin and M. Matsuazawa, J. Phys. B **29**, L389 (1996).
[23] M. Pieksma, M. Gargaud, R. McCarroll, and C. C. Havener, Phys. Rev. A **54**, R13 (1996).
[24] T. G. Lee, M. Hesse, A. T. Le, and C. D. Lin, Phys. Rev. A **70**, 012702 (2004).